# An Exploratory Optimal Framework of Low Impact Development Measures Spatial Arrangement based on Source Tracking for Urban Flood Mitigation

**Wenchao Qi**
Tianjin University
**Chao Ma** ( mac_tju@126.com )
Tianjin University
**Hongshi Xu**
Zhengzhou University
**Zifan Chen**
Tianjin University
**Kai Zhao**
Tianjin University
**Hao Han**
Xi'an University of Technology

**Research Article**

**Keywords:** Low impact development, Regional relevance, Source tracking, Spatial arrangement, Urban flood model

**Posted Date:** March 23rd, 2021

**DOI:** https://doi.org/10.21203/rs.3.rs-350792/v1



**Version of Record:** A version of this preprint was published at Water Resources Management on August 4th, 2021. See the published version at https://doi.org/10.1007/s11269-021-02915-2.

# An exploratory optimal framework of low impact development measures spatial arrangement based on source tracking for urban flood mitigation

Wenchao Qi [1,2], Chao Ma [1,2*], Hongshi Xu [3], Zifan Chen [1,2], Kai Zhao [1,2], Hao Han [4]

[1]State Key Laboratory of Hydraulic Engineering Simulation and Safety, Tianjin University, Tianjin 300072, China

[2]School of Civil Engineering, Tianjin University, Tianjin 300072, China

[3]School of Water Conservancy Engineering, Zhengzhou University, Zhengzhou, 450001, China

[4]State Key Laboratory of Eco-hydraulics in Northwest Arid Region of China, Xi'an University of Technology, Xi' an 710048, China

* Corresponding author: Chao Ma

E-mail addresses: mac_tju@126.com (C. Ma)

**Abstract:** Urban areas are vulnerable to flooding as a result of climate change and population growth and thus rainstorm-induced flood losses are becoming increasingly severe. Low impact development (LID) measures are a storm management technique designed for controlling runoff in urban areas, which is critical for solving urban flood hazard. Therefore, this study developed an exploratory simulation-optimization framework for the spatial arrangement of LID measures. The proposed framework begins by applying a numerical model to simulate hydrological and hydrodynamic processes during a storm event, and the urban flood model coupled with the source tracking method was then used to identify the flood source areas. Next, based on source tracking data, the LID investment in each subcatchment was determined using the inundation volume contribution ratio of the flood source area (where most of the investment is required) to the flood hazard area (where most of the flooding occurs). Finally, the resiliency and sustainability of different LID scenarios were evaluated using several different storm events in order to provide suggestions for flooding predictions and the decision-making process. The results of this study emphasized the importance of flood source control. Furthermore, to quantitatively evaluate the impact of inundation volume transport between subcatchments on the effectiveness of LID measures, a regional relevance index (*RI*) was proposed to analyze the spatial connectivity between different regions. The simulation-optimization framework was applied to Haikou City, China, wherein the results indicated that LID measures in a spatial arrangement based on the source tracking method are a robust and resilient solution to flood mitigation. This study demonstrates the novelty of combining the source tracking method and

highlights the spatial connectivity between flood source areas and flood hazard areas. Further, the framework acts as a strategic tool for the effective spatial arrangement design of LID measures.

**Keyword:** Low impact development, Regional relevance, Source tracking, Spatial arrangement, Urban flood model

## 1 Introduction

Hydrological responses are significantly affected by interactions between the temporal and spatial variability of rainfall, and watershed characteristics. These interactions are extremely pronounced in urban areas, where runoff generation is quick because of the high degree of impervious cover (Cristiano et al. 2019). Thus, urban flood has become a global issue as the result of climate change, urbanization, and urban drainage infrastructure limitations (Duan et al. 2016; Tang et al. 2016; Wang et al. 2019; Valizadeh et al. 2019), thereby causing significant impacts on society, the economy, and the environment. Several trends indicate that urban flood hazard will only increase with time. First, as climate change has increased the extreme rainfall events, both by frequency and magnitude. An increase in extreme rainfall events, particularly high intensity short duration rainfalls, has been observed as of late (Willems et al. 2012). Climate change has been widely acknowledged as a serious issue because of its impact on urban areas in terms of changes in runoff (Ranger et al. 2011; Hallegatte et al. 2011). Second, the urban population is projected to will exceed 80% of the total population by 2030 (Salvadore et al. 2015), thereby exposing more people to flooding. Further, as urbanization is expanding to accommodate increasing populations, the transition of

natural catchments into urbanized catchments causes urban flood through reduced infiltration and faster hydrological responses (Becker et al. 2018). Third, corresponding to the transformation of rural landscape into urban forms, an obvious relationship between local micro-climates and urban areas has developed. This relationship promotes the occurrence of urban flood. For example, the “urban heat island” effect, wherein urban areas have higher temperatures than surrounding regions, has been well proposed (Bentley et al. 2010). In some cases, “urban heat island” increases rainfall volume in regions downwind of urban areas. Without interference, the damage caused by flood globally may increase by up to a factor of 20 by the end of the century (Winsemius et al. 2016).

Impermeability and the rapid transportation of stormwater are both linked to a drastic reduction in the hydrologic function of the landscape, including infiltration and evapotranspiration result in typical consequences are high flow peaks, rapid runoff movement, and high frequency flooding. Low impact development (LID) measures, which is a storm management and non-point source pollution treatment technique, was first adopted in North America and New Zealand in the 1980s (Fletcher et al. 2015). It aims to control the runoff and pollution generated by storm events via a decentralized and small-scale source control to ensure that the development area is as similar as possible to the natural hydrological cycle. Furthermore, LID measure is an ecological technique that can easily realize urban stormwater collection and utilization. In particular, it emphasizes the on-site small-scale control of stormwater sources. For example, Hood et al. (2007) compared the effects of LID and traditional residential

development, and the results found that LID lowered runoff volume, the runoff coefficient, peak discharge rate. It also indicated that the LID effect was even greater for smaller storms with shorter durations. Williams et al. (2006) compared four development alternatives for infiltration techniques and land preservation to indicate that LID measure is effective for small storms. LID planning and implementation for urban flood mitigation have thus been proposed as an indispensable component of urban stormwater management. Selecting a proper spatial arrangement of LID measures and placing them in the suitable location is crucial when designing LID measures spatial layout schemes under given investment constraint. As policymakers are concerned about how to achieve a positive multi-functional return, especially regarding the flood hazard aspects. Thus, there is an urgent need to reach a balance between economic issues and LID spatial allocation.

Some studies have indicated that scenario analysis methods for LID spatial arrangement design can address these concerns. Scenario analysis methods are driven by a set of influencing factors, wherein each planning scenario is designed based on certain prerequisites. For example, Liu et al. (2014) quantitatively assessed the flood peak flow reduction of Green Infrastructure (GI), and the results showed that integrated GIs spatial arrangement is more effective than single measure for flood mitigation. Gilroy et al. (2009) conducted a study to determine the impact of LID measures on reducing flooding. They indicated that flood reduction capacity of single LID measure is determined by the potential mechanism, and the spatial arrangement of the measure greatly affects the flood control effectiveness of multiple LID measures. However, the

111 quality of scenario assumptions greatly influences the reliability of scenario analysis
112 (Urich, et al. 2014; Zischg, et al. 2017). In addition, the inability to identify all potential
113 scenarios, scenario analysis does not seek the most cost-effective solutions, which often
114 result in schemes far from pareto optimality (Liu et al. 2016; Xu et al. 2017).

115 The shortcomings of scenario analysis methods have led to many researchers to
116 design LID measures spatial arrangement based on urban flood models coupled with
117 optimizing algorithm. An optimizing algorithm is a powerful technique with general
118 applicability for solving multi-objective problems with several contradictory objectives.
119 The constraint factors for optimization primarily involve three themes (Bakhshipour et
120 al. 2019): (1) design objectives, such as the reductions in runoff and peak flow volume;
121 (2) site characteristics, such as the degree of urbanization, topography, climate features,
122 and land use; and (3) the cost of LID measures. The results of LID optimization provide
123 policymakers with a design and planning method that can achieve the optimal balance
124 of decentralized detention while considering flood disaster control, peak flow reduction,
125 and investment cost. For example, In order to minimize downstream flood peak flow,
126 Liang et al. (2019) adopted the SWMM coupled with a genetic algorithm to determine
127 the optimal LID spatial arrangement. Huang et al. (2018) combined the Simulated
128 Annealing algorithm with SWMM to investigate the optimization of the LID spatial
129 arrangement while considering the benefit-cost ratio. Cano et al (2016) adopted a multi-
130 objective optimization algorithm to analyze spatial arrangement of LID measures for
131 stormwater management. The results indicated that in terms of cost-benefit ratio,
132 implementing LID measures in upstream areas is the most effective approach.

Optimization allows researchers to identify the optimal solution set from a large number of results. However, some research gaps remain. First, as an optimization model is a "black-box" approach, it lowers the confidence of city planners in the optimization results. Second, optimization often leads to non-unique solution sets. Third, previous studies mostly focused on coupled simulation-optimization methods, which normally require large computational burdens (particularly for two-dimensional flood modeling). Thus, it is desirable to develop more efficient ways of conducting evaluations and future designs. In addition, traditional multi-objective evolution algorithms and scenario analysis methods can not determine the most effective spatial arrangement of the LID measures.

A city is a complex space formed by the interaction of multiple interoperable catchments, in which water is central to many of these interactions as it can be transported to different subcatchments via flood pathways. An obvious disconnect between the most effective locations for flood management investments and the locations where floods are most likely to occur. While researches exist regarding the selection of LID measures depending on a specific location, they usually obtain information regarding only one aspect of urban flooding such as traffic channel or infrastructure that may be at risk. There are few methods that link the root causes and potential impacts of flood problems to specific flood management interventions within existing urban systems. Therefore, identifying flood source areas (i.e., target locations that have the greatest impact on reducing flood hazards) can help guide the spatial priority of flood management measures. For this purpose, an exploratory analysis

framework was proposed that aims to guide strategic decision-making for LID measures spatial arrangement designs. This framework involves a methodological process that combines flood mitigation strategies with spatial connectivity and uses the regional relevance index (*RI*) to quantitatively measure the connection between flood source areas and flood hazard areas based on source tracking. By applying this framework to the urban watershed of Haikou (China), we identified the potential prioritization of LID spatial arrangement using source tracking data as a driving force. Furthermore, the framework output is especially important as it highlights the spatial connectivity between the flood source area (requiring most of the LID measures) and the beneficiary area (the areas where flooding is mostly reduced), thereby creating a basis for strengthening cooperation between these areas.

## 2 Materials and methods

### 2.1 Overall framework

The overall framework of the proposed method is illustrated in Fig. 1. First, an urban flood coupled model was established using a hydraulic model, hydrologic model, and source tracking module. Second, using a coupled model, the inundation volume was simulated under typical scenarios combining rainfall and tide level. Third, according to the inundation volume, the regional flood transfer coefficient (*A*) and *RI* were calculated for the drainage district. Finally, the spatial arrangement ratio for LID measures in different subcatments is determined by *A* and LID investment ratio (*KI*), and efficacy evaluation of adaptive LID measures are proposed for different LID scenarios.

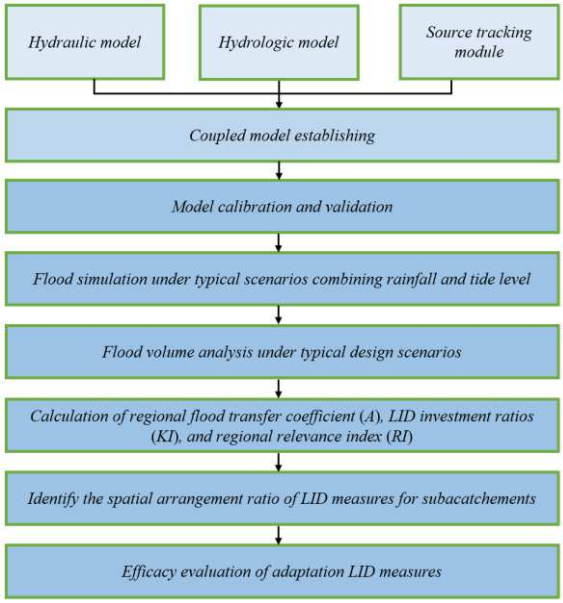


**Fig. 1** Optimal framework of spatial arrangement of low impact development (LID) measures based on source tracking for urban flood mitigation

## 2.2 Source tracking method based on PCSWMM model

### 2.2.1 Source tracking method

The source tracking method depends on the relationship of a certain tracer with a specific host, wherein the origin of the host can be defined. In this study, tracers were employed to trace the entire process of stormwater runoff between different subcatchments in order to obtain the composition and source contribution of the inundation volume. According to the composition of the inundation volume in the hazard areas, an allocation scheme of LID measures can be developed to achieve the optimal urban flood mitigation strategy.

For example, during a storm event, the urban watershed (as shown in Fig. 2), which consists of three subcatchments (*S1*, *S2*, and *S3*), can flood in response to rapid runoff. The arrows represent the preferred direction of water flow. The runoff generated by subcatchment *S1* flows into *S2* and is mixed with the inundation volume generated

by *S2*. Subsequently, the inundation volume of *S2* divides into two parts. Some of the water flows into *S3*, while the rest remains in *S2*. Accordingly, the inundation volume of the flood hazard area is composed of the runoff of each subcatchment. We evaluated the runoff from subcatchments *S1*, *S2*, and *S3* using tracers A, B, and C, respectively, of constant concentration. According to the conservation of mass equation, the cumulative inundation volume from subcatchment *S1* in the hazard area expresses the ratio of the mass of tracer A to the corresponding concentration, as described in Eq. (1). Although the urban watershed is much more complex than the area in Fig. 2, the calculation method of the conservation relationship between inundation volume and tracer transfer is still effective, as given by Eq. (2).


**Fig. 2** Schematic diagram of the runoff source tracking process in urban watershed

$$\begin{cases} \dfrac{C_1V_1}{V_1+V_2+V_3}=C_1' \\ \dfrac{C_2V_2}{V_1+V_2+V_3}=C_2' \\ \dfrac{C_3V_3}{V_1+V_2+V_3}=C_3' \end{cases} \tag{1}$$

where $C_1$, $C_2$, and $C_3$ are the initial tracer concentrations for subcatchments *S1*, *S2*, and *S3*, respectively, which are constant values. $C_1'$, $C_2'$, and $C_3'$ are the concentrations of tracers in the flood hazard areas, and $V_1$, $V_2$, and $V_3$ represent the amount of inundation

volume contributed by the three subcatchments (i.e., flood source areas) to the flood hazard areas, respectively.

$$\begin{cases} \dfrac{C_1V_1}{V_1+V_2+\cdots\cdots+V_n}=C_1' \\ \dfrac{C_2V_2}{V_1+V_2+\cdots\cdots+V_n}=C_2' \\ \cdots\cdots \\ \dfrac{C_nV_n}{V_1+V_2+\cdots\cdots+V_n}=C_n' \end{cases} \tag{2}$$

where $C_1$, $C_2$,….$C_n$ are the initial tracer concentrations for subcatchments *S1*, *S2,* ….*Sn*, which are constant values. Meanwhile, $C_1'$, $C_2'$, …$C_n'$ are the concentrations of tracers in flood hazard areas, and $V_1$, $V_2$,….$V_n$ represent the amount of inundation volume contributed by the 1–*n* subcatchments (i.e., flood source areas) to the flood hazard areas, respectively.

### 2.2.2 PCSWMM

The PCSWMM combines SWMM 5 and GIS to provide a complete package for one-dimensional and two-dimensional analyses of stormwater modeling in urban watersheds (Tillinghast et al, 2012; Ahiablame et al, 2016; Xu et al 2018). The PCSWMM can accurately simulate unsteady two-dimensional surface flow above ground via two-dimensional floodplain modeling. The one-dimensional conduit and two-dimensional floodplain models were integrated by using the orifice connection method (Xu et al 2018). The hydraulic simulation calculation of drainage conduit was performed by adopting the dynamic wave method. In general, the drainage network system and water supply network form a set of urban water simulation systems. The basic principles of the model are the continuity and momentum equations as follows (Xu et al 2018):

$$\frac{\partial A}{\partial t}+\frac{\partial Q}{\partial l}=0 \tag{3}$$

$$\frac{\partial Q}{\partial t}+\frac{\partial\left(Q^2 / A\right)}{\partial l}+gA\frac{\partial H}{\partial l}+gAS_f+gAh_L=0 \tag{4}$$

where $A$ represents the cross-sectional area ($m^2$), $l$ represents the distance along the conduit (m), $Q$ represents the flow rate ($m^3/s$), $t$ represents time (s), $H$ represents the pressure head (m), and $h_L$ represents the local energy loss/unit length conduit (m), $S_f$ represents the friction slope, $g$ represents the gravitational acceleration ($m/s^2$).

In the PCSWMM, water quality routing within the conduit links and nodes assumes that the behavior of a continuously stirred tank reactor, and the concentration of a constituent exiting the conduit at the end of a time step is determined by integrating the conservation of mass equation, using average values for quantities that might change over time, such as the flow rate and conduit volume (CHI 2014). In this study, the event mean concentration (EMC) washoff model in the PCSWMM was adopted to generate a tracer source with a constant concentration. The EMC model is described by Eq. (5). Because the tracer only distinguishes the inundation volume, the tracer concentration settings in different subcatchments are the same. In the EMC model, the generation and disappearance of tracers occurs synchronously with the runoff process, and the total mass of the tracers is proportional to the cumulative runoff. In addition, the total mass of the tracer remains constant even though its concentration and spatial distribution changes during flow movement. Within the PCSWMM, the grid inundation volume and tracer concentration processes can be obtained, and the inundation volume transfer process can be calculated using Eq. (2).

$$EMC = \frac{\int_0^T C_t Q_t dt}{\int_0^T Q_t dt} \tag{5}$$

where EMC is the event mean concentration (mg/L), $T$ is the total runoff time, $C_t$ is the pollutant concentration (mg/L), which varies with runoff time, and $Q_t$ is the runoff flow (L/s), which varies with runoff time.

## 2.3 Adaptive LID spatial arrangement scheme

### 2.3.1 Quantifying the regional relevance

The inundation volume contribution from the source area can be quantified using the source tracking data. If the inundation volume in the hazard area comes from multiple subcatchment runoffs, then the regional relevance is strong. Conversely, if the inundation volume comes from a smaller number of subcatchments, the regional relevance is weak. To quantify regional relevance, the regional relevance index (*RI*) was developed to determine the importance of inundation volume transfer between flood source and hazard areas during urban flood mitigation. The following method can be adopted to quantify the *RI* for coastal cities. First, the regional flood transfer coefficient (*A*) is calculated as follows:

$$A_{i,j} = \frac{\sum_{t=0}^{t=n} \left(V_{i,j}\right)_t}{\sum_{t=0}^{t=n} \left(W_{i,j}\right)_t} \tag{6}$$

where $V_{i,j}$ and $W_{i,j}$ are the transferred and generated inundation volumes, respectively, in an urban watershed under different combinations of rainfall and tide levels. $i$ and $j$ represent the design return periods of the rainfall and tide levels, respectively, and $t$ represents the time step of the flood simulation.

However, the calculation of $A_{i,j}$ must be adjusted as the design periods of rainfall and tide levels do not coincide, and the revision can be resolved in two cases.

(1) Regarding rainfall, the following revision should be included:

$$C_1 = (A_{1,1} + A_{1,2} + \cdots\cdots A_{1,n}) / n \tag{7}$$

$$C_2 = (A_{n,1} + A_{n,2} + \cdots\cdots A_{n,n}) / n \tag{8}$$

$$\beta = \frac{C_2 - C_1}{h_n - h_1} \tag{9}$$

$$\begin{cases} p_{i,j} = A_{i,j} + \beta(h_j - h_i) & i < j \\ p_{i,j} = A_{i,j} & i = j \\ p_{i,j} = A_{i,j} - \beta(h_i - h_j) & i > j \end{cases} \tag{10}$$

$$p_1 = \frac{\sum_{i=1}^{n}\sum_{j=1}^{n} p_{i,j}}{n^2} \tag{11}$$

where $A_{1,1}$, $A_{1,2}$…$A_{1,n}$ are calculated using Eq. (6) when the cumulative rainfall volume is $h_1$ (the minimum design rainfall volume), and the cumulative tide level changes from $z_1$ (the minimum design tide level) to $z_n$ (the maximum design tide level). Further, $\beta$ represents the unit change in rainfall, $p_{i,j}$ represents the revision value of $A_{i,j}$ in the rainfall changes, and $p_1$ is the average revision value under different combinations of rainfall and tide levels.

(2) Regarding tide level, the revision is defined as follows:

$$C_3 = (A_{1,1} + A_{2,1} + \cdots\cdots A_{n,1}) / n \tag{12}$$

$$C_4 = (A_{1,n} + A_{2,n} + \cdots\cdots A_{n,n}) / n \tag{13}$$

$$\gamma = \frac{C_4 - C_3}{z_n - z_1} \tag{14}$$

$$\begin{cases} q_{i,j} = A_{i,j} - \gamma(z_j - z_i) & i < j \\ q_{i,j} = A_{i,j} & i = j \\ q_{i,j} = A_{i,j} + \gamma(z_i - z_j) & i > j \end{cases} \quad (15)$$

$$q_1 = \frac{\sum_{i=1}^{n}\sum_{j=1}^{n} q_{i,j}}{n^2} \quad (16)$$

where $A_{1,1}$, $A_{2,1}$…… $A_{n,1}$ are calculated using Eq. (6) when the cumulative tide level value is $z_1$ (the minimum design tide level), and the cumulative rainfall volume changes from $h_1$ (the minimum design rainfall volume) to $h_n$ (the maximum design rainfall volume). In addition, $\gamma$ represents the unit change in design tide level, $q_{i,j}$ represents the revision of $A_{i,j}$ in the design tide level changes, and $q_1$ is the average revision value under different combinations of rainfall and tide levels. Thus, the *RI* is determined as follows:

$$RI = \frac{q_1 + p_1}{2} \quad (17)$$

### 2.3.2 Spatial arrangement ratio for LID measures

Using the urban flood model, the inundation volume of each subcatchment can be calculated under different combinations of rainfall and tide levels. Further, the inundation volume contribution from the source area can be quantified based on the source tracking data. Then, the scale of the LID measures in different subcatchments is determined according to the ratio of each subcarchment's inundation volume contribution to the flood hazard area, which indicates that LID measures in larger innundation volume contribution areas have larger area ratios. The inundation volume contribution ratios of different subcatchments to the flood hazard area are determined as the investment ratio of the LID measures. This means that the inundation volume

contribution proportion of each subcatchment to the flood hazard area is equivalent to the investment proportion of LID measures in each subcatchment. Eq. 6 can be used to calculate the *A* under different return periods of rainfall at certain tide levels. The rainfall and tide level values with the maximum *A* were used as inputs for the flood model to calculate the LID investment ratios (*KI*) of different subcatchments. To reduce the flood risk of the entire study area, we defined the flood hazard area as the entire study area. The following method can be adopted to quantify the flood contribution ratio and:

$$KI_k = \left( \frac{\sum_{t=0}^{t=n} \left(T_{i,j}\right)_t}{\sum_{t=0}^{t=n} \left(W_{i,j}\right)_t} \right)_k \tag{18}$$

where $(T_{i,j})_k$ is the inundation volume contribution produced by the subcatchment $k$ to the entire area, and $W_{i,j}$ is the inundation volume of the entire study area. The return periods of the designated rainfall ($i$) and tide level ($j$) are based on the maximum *A* calculated using Eq. 6.

A comprehensive cost and benefit analysis is required to determine the LID allocation. In this work, the benefits can be defined as inundation volume reduction due to implementation of flood mitigation strategies. Based on the source tracking method, LID investment in each subcatchment was determined by the inundation volume contribution ratio of the source area to the hazard area, especially within strict budgetary constraints.

Generally, the larger the ratio of flood mitigation projects, the higher the total volume detained, the stronger the flood reduction, and thus, the higher the cost. Eqs.

329 (19)–(21) were adopted to identify the urban flood mitigation plans at a budget
330 constraint.

331 $$C_k = C_{total} \times KI_k \tag{19}$$

332 $$C_k = \sum_{i=1}^{N} P_k \times C_P \tag{20}$$

333 where $P_k$ is the area of the LID measures in subcatchment $k$, which was retrofitted with
334 the LID measure, $C_p$ is the cost of unit area of the LID measure, and $C_{total}$ represents the
335 total implementation investment of the flood management strategies. Eq. (21) describes
336 the reduction in peak flow as a result of the LID solution compared with existing or
337 predevelopment conditions.

338 $$R = 100 \times \left( \frac{V_{Before} - V_{After}}{V_{Before}} \right) \% \tag{21}$$

339 where $V_{Before}$ is the change in peak inundation volume associated with the designated
340 storm event, and $V_{After}$ is the peak flow volume after the implementation of flood
341 mitigation measures. The resilience of each optimized scheme with different flood
342 mitigation strategies was evaluated using the indicator $R$.

343 **3 Case study**

344 **3.1 Coupled urban flood model with source tracking method in Haikou City**

345 **3.1.1 Study area**

346 The main districts of Haikou City (Fig. 3) were selected as the study area. The
347 urban watershed is located in the north of the Hainan Province, which is adjacent to the
348 Qiongzhou Strait. The land use types in the main districts of Haikou City are mainly
349 homes, roads, and buildings, resulting in a high ratio of impermeable areas. The annual

average temperature and rainfall are 24.3 °C and 2067 mm, respectively, which is a typical of tropical oceanic monsoon climate. The study area is vulnerable to urban flooding because of its high population density and flat terrain. For example, the occurrence of typhoon “Rammasun” during July 17–19, 2014, resulted in heavy rainfall on July 18, causing eight deaths and losses worth nearly 9 billion yuan.

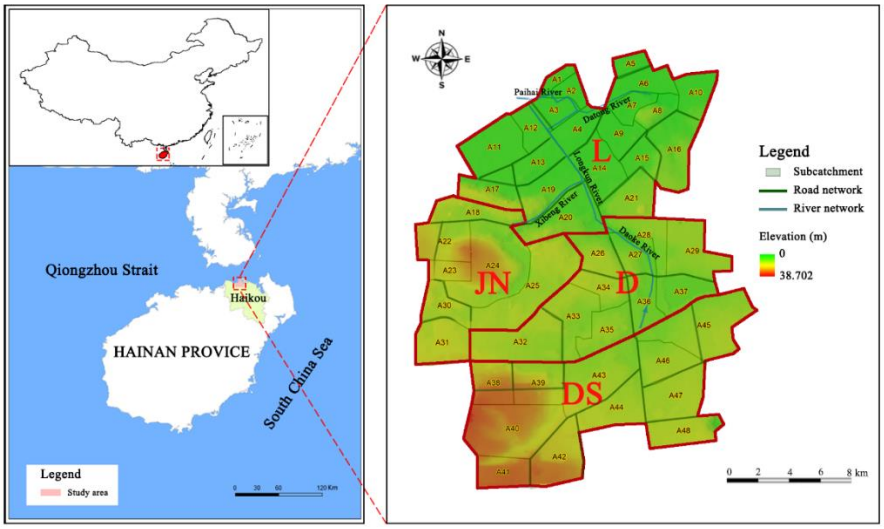


**Fig. 3** Study area and sewer system distribution

### 3.1.2 Establishing coupled model in Haikou City

The data adopted for the urban flood model included rainfall, tide level, digital elevation model data, river data, and pipe network data, which were provided by the Haikou Municipal Water Authority. The urban flood model (Fig. 4) comprised 4401 links, 4563 nodes, 4 catchments, and 48 subcatchments. The subcatchment areas ranged in size from 14.76 ha to 136.35 ha. The total contributing area of the subcatchments was 2770.84 ha, of which 2042.93 ha was classified as impermeable and 727.91 ha as pervious. A recorded historical extreme precipitation event that occurred during July 17–19, 2014 resulted in a heavy flood hazard. Based on the measured rainfall data from 1974 to 2012 derived by the Haikou Station, the rainfall and tide level distributions (Fig.

5) were fit with a Pearson type-III (P-III) distribution, and return periods of 2 years, 10 years, and 20 years were adopted as model inputs to analyze the flood response.

The source tracking method in the PCSWMM adopted the EMC washoff model, which can generate a stable tracer source for overland flow. The source tracing method only marks the amount of runoff in different subcatchments. Note that the washoff coefficient value in PCSWMM was set to be the same for all subcatchments, and other parameter values were set to 0.

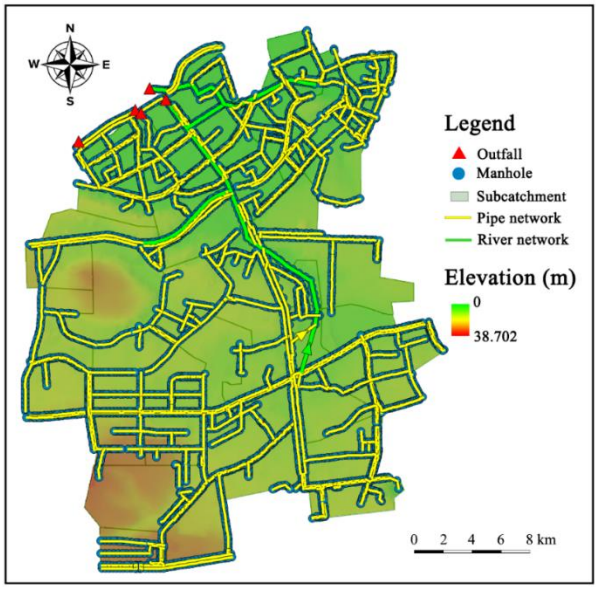


**Fig. 4** Urban flood model establishing of study area based on the PCSWMM

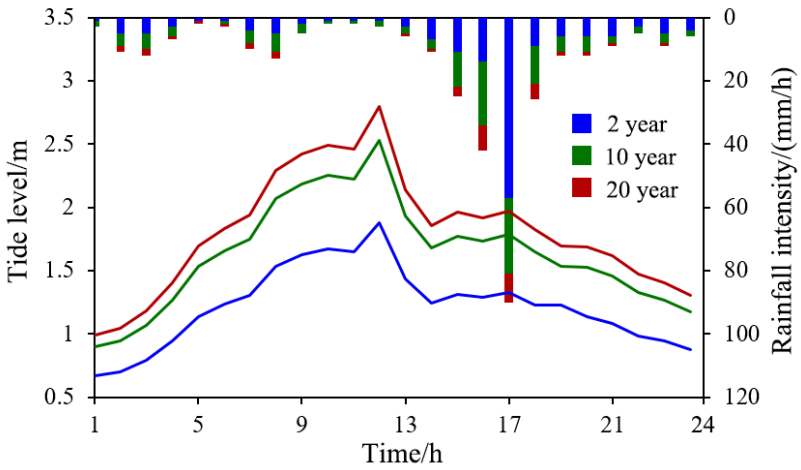


**Fig. 5** Distribution of design rainfall and tide level

### 3.1.3 Model calibration and validation

The parameters of the urban flood coupled model established by PCSWMM were calibrated by trial and error method. The Nash–Sutcliffe efficiency (NSE) index was used to measure the goodness of fit between the observation and simulation inundation depth values to evaluate the accuracy of the coupled model. In this study, the calibration inundation data were acquired during the typhoon "Rammasun" event. The comparison of simulated and measured inundation depth is shown in Figure 6. The observation locations are shown in Figure 7. The error between the observation and simulation values was less than 0.1 m, and the NSE value was 0.844. When the NSE value is greater than 0.5, the simulation results are satisfactory (Ahiablame et al. 2016). Hence, the coupled model is feasible and can be used to simulate a given flood scenario.

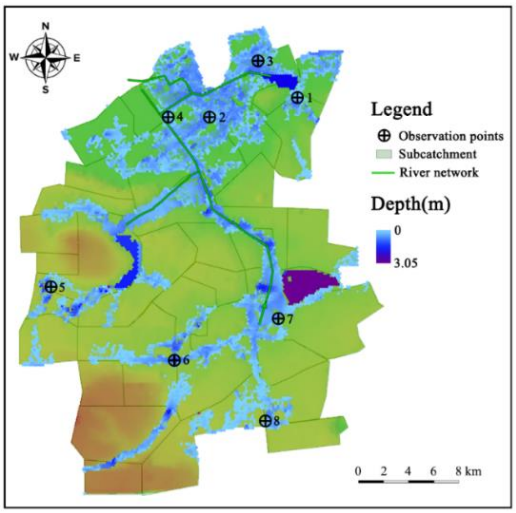


**Fig. 6** Simulation flood during the "Rammasun" typhoon storm event in July 2014

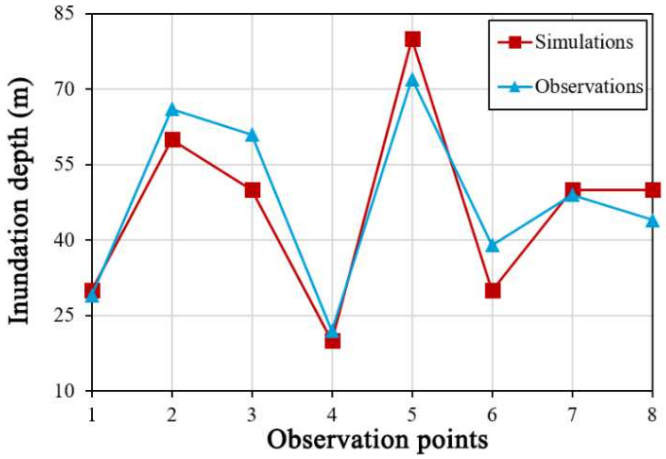


**Fig. 7** Calibration of the PCSWMM

### 3.2 Flood simulation in compounding rainfall and storm tide events

The total inundation volumes, which can numerically reflect holistic severity, were obtained during the simulation period. Based on source tracking method, the inundation volume source of the entire study area is divided into 4 catchments (namely, L, JN, D, and DS), wherein the related inundation volume process is shown in Fig. 8. It shows that the contribution ratio of the source inundation volume in the catchment varied. For example, when the return periods of rainfall and tide level were both set to 20-year, the peak inundation volume contribution ratios of the catchments L, JN, D, and DS were 28.90%, 40.44%, 11.32%, and 19.34%, respectively. Hence, regarding the flood disaster reduction strategies, it is necessary to focus on the source flood control of catchments JN and L.

In addition, the design values of rainfall and tide levels also affected the contribution ratio. For example, during the compound storms of 2-year rainfall with 2-year, 10-year, and 20-year tide, the inundation volume contribution ratios of catchment JN were 53.91%, 53.33%, and 51.35%, respectively. Furthermore, the inundation volume contribution ratios of catchment JN were 53.91%, 44.40%, and 42.29% for a

2-year tide period with compound rainfall periods of 2-year, 10-year, and 20-year, respectively. These results indicate that, compared with the tide level, change in rainfall has a greater impact on inundation volume generation in the flood source area of catchment JN.

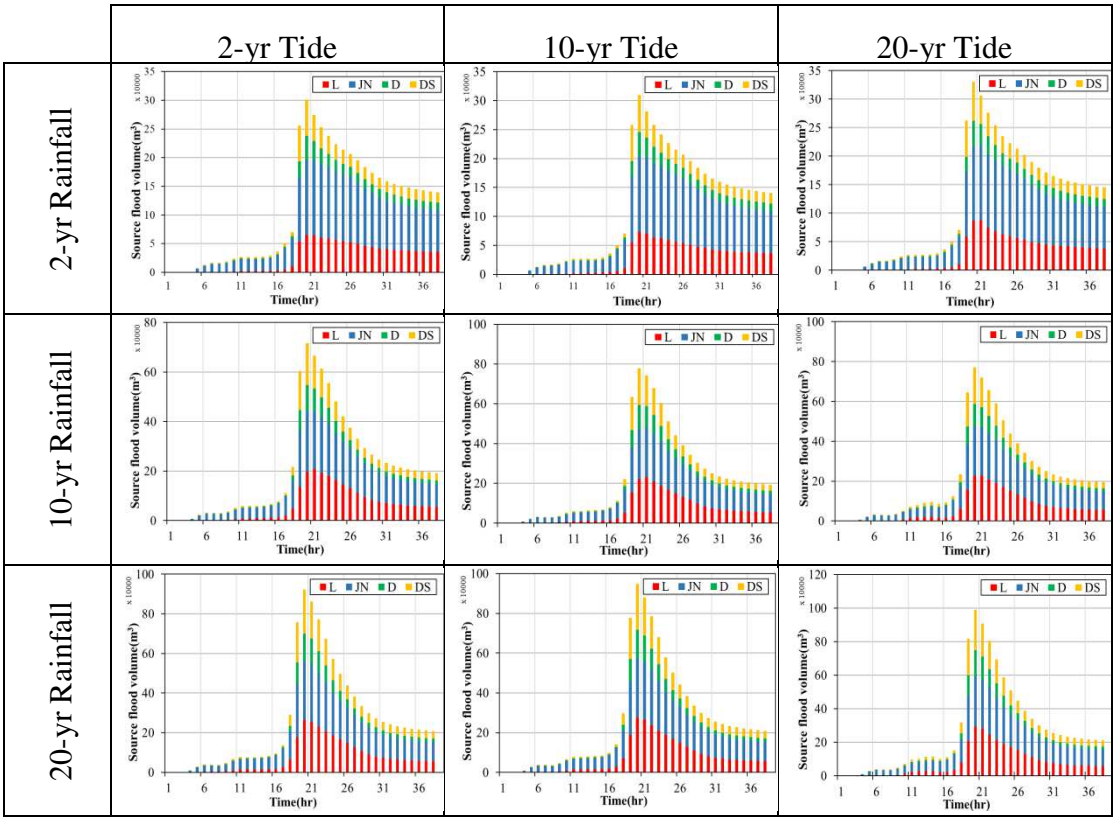


**Fig. 8** Diagram of flood source area inundation volume contribution to hazard area under the combined impact of storm tides and heavy rainfall

### 3.3 Quantification analysis of regional relevance

An urban flood model was used to simulate flood processes under the combined impact of storm tides and heavy rainfall, wherein source tracking data were used to determine the source of flooding in a disaster area. The regional flood transfer coefficients calculated using Eq. (6) are listed in Table 1. The results indicate that the regional flood transfer coefficient increases with increasing rainfall return period and

tide level. Specifically, for a return rainfall period of 2 years with 2 years, 10-year, and 20-year tide level return, the values of $A$ were 0.347, 0.349, and 0.352, respectively. Further, at a return tide level period of 2 years, and return rainfall periods of 2 years, 10 years, and 20 years, the values of $A$ were 0.347, 0.368, and 0.392, respectively. These results show that, compared with tide level, rainfall change has a greater impact on inundation volume generation in the regional flood transfer coefficient.

Using Eqs. (7)–(17) to revise the inconsistency between rainfall and tide levels, the RI of the study area was found to be 0.375, indicating that 37.5% of the inundation volume in the study area realized cross-regional transfer under stormwater events. This emphasizes the importance of source flood control in urban flood mitigation strategies.

**Table 1** Regional flood transfer coefficients ($A$) under combined storm tide and heavy rainfall periods

| Design Return period | 2-yr design rainfall | 10-yr design rainfall | 20-yr design rainfall |
|---|---|---|---|
| 2-Yr design tide level | 0.3474 | 0.3685 | 0.3922 |
| 10-Yr design tide level | 0.3493 | 0.3844 | 0.3934 |
| 20-Yr design tide level | 0.3522 | 0.3889 | 0.3994 |

### 3.4 Simulation scenarios

Herein, we simulated the placement of permeable pavement that increases on-site

storage as the water slowly penetrates into the underlying soil, the water is stored in a highly permeable matrix. The cost of implementing flood mitigation technologies varies considerably based on certain system specifications, soil type, and the location of implementation. Therefore, this study selected a representative cost of 194 yuan/$m^2$ for installing permeable pavement (Hong et al. 2020). The total LID cost was selected to be 1 billion yuan, which is equivalent to a two-year government investment in a single pilot area of the "Sponge city" program construction in China.

A series of scenarios were explored to determine the placement of LID solutions for various storm events and budget constraints in main districts of Haikou City. Moreover, the analysis explored the varying limitations of the budget for effective stormwater control. Considering the essential difference between the flood source and flood hazard areas, two modes of intervention were designed:

A1–Without interventions, reflecting the actual state of flooding in the urban watershed.

A2–Local control interventions based on the inundation volume ratio of the flood hazard area.

A3–Source control interventions based on the inundation volume ratio of the flood source area to the flood hazard area.

Because of investment constraints, policymakers should allocate LID measures effectively to alleviate flooding. Hence, a spatial arrangement framework with the ability to mitigating the inundation volume was proposed to determine the optimal layouts of LID measures. In the spatial arrangement framework, the objective is to

mitigating the inundation volume in the watershed within the budget constraints under the worst designed storm. The use of LID measures is considered in the allocation framework by dividing the catchments into subcatchments to determine the LID ratios of each subcatchment.

According to the three LID measure scenarios, different spatial arrangement schemes were developed. The A2 scenario is based on flood hazard area control, wherein the ratios of the LID measure investment in four catchments are equivalent to the ratios of inundation volume of each catchment to the inundation volume of the entire study area. Meanwhile, the A3 scenario is determined by flood source area control, which is based on source tracking data, wherein the inundation volume of the entire study area is distinguished by the source of inundation, and the source inundation volume contribution ratios of the four catchments to the study area are determined to be the investment ratio of the LID measures in each catchment. Each scenario was simulated during the compound storm of 20-year rainfall with 20-year tide (designing scenario under maximum *A* value). The LID measures and the spatial arrangement ratios in scenarios A2 and A3 are summarized in Table 2.

**Table 2** Low impact development (LID) ratio for scenarios A2 and A3

| Location | %Allocation | | | |
|---|---|---|---|---|
| | Scenario A2 | | Scenario A3 | |
| | LID area ratio | Investment percentage | LID area ratio | Investment percentage |
| Catchment L | 47.59% | 61.04% | 22.53% | 28.90% |
| Catchment JN | 18.09% | 13.40% | 54.57% | 40.44% |
| Catchment D | 18.84% | 15.96% | 13.35% | 11.32% |
| Catchment DS | 7.64% | 9.60% | 15.42% | 19.34% |

### 3.5 Efficacy evaluation of adaptive LID measures

To alleviate the urban flooding under different return periods, LID measures were determined for two scenarios (Fig. 9). The results show that LID effects vary with the return period of stormwater events. Specifically, the peak inundation volume reduction rate increases when the storm events are less intense. Compared with the A1 scenario, LID measures can reduce the peak inundation volume by 11.42%–25.04%, 24.59% – 32.48%, respectively. In general, the efficiency of the hazard inundation volume reduction was as follows: scenario A1< scenario A2< scenario A3.

Furthermore, with increasing return period, the effective reduction rate of scenario

A3 was higher than that of scenario A2. At the return periods of 2 years, 10 years, and 20 years, scenario A3 reduced the peak inundation volumes by 7.44%, 9.03%, and 13.17%, respectively, as compared with those of scenario A2. This is because with increasing design return period, the *RI* increases, thereby increasing the regional inundation volume transfer ratio, which makes the flood source area control strategy more effective. This validates the effectiveness of the proposed framework.

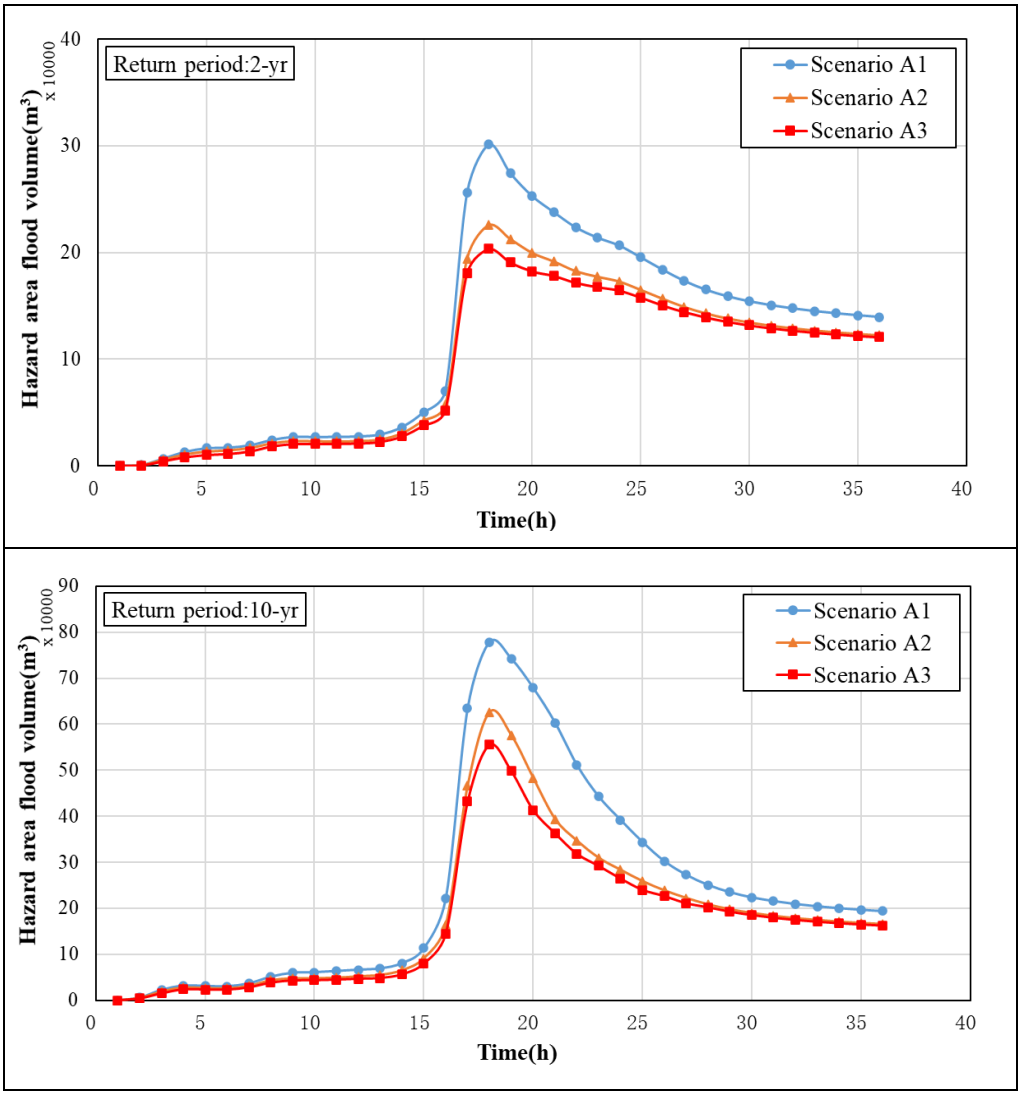

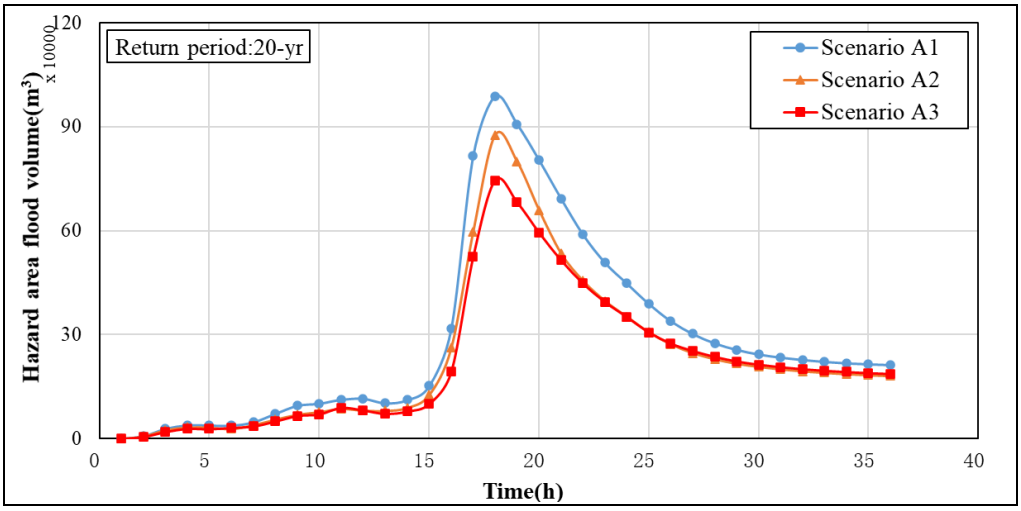


**Fig. 9** Comparative diagram of inundation volumes in three scenarios during combined storm tide and heavy rainfall

## 4 Conclusions

In this study, a simulation-optimization framework for designing LID strategies that utilizes the source tracking technique was proposed. The framework was successfully applied to Haikou City, and the results revealed the importance of the spatial connectivity of LID measures. The main conclusions are as follows:

- The framework first introduced the source tracking method in LID measure spatial arrangement, based on source tracking data in order to distinguish the source of the hazard area inundation volume and determine an LID allocation strategy according to the flood contribution ratio of the flood source area. These findings are especially important for highlighting flood source control to mitigate urban flood hazards.
- To quantify regional relevance, a regional relevance index (*RI*) was developed to determine the importance of inundation volume transfer between flood source and hazard areas during urban flood mitigation. These results show that the regional inundation volume transfer greatly impacts the efficacy of LID measures.

Furthermore, different disaster-causing factors have different degrees of impact on the regional correlation indicators. Moreover, compared with the tide level, the *RI* is more sensitive to rainfall volume, wherein the greater the rainfall intensity, the higher the *RI* in different regions.

- For different design return period storm events, the effectiveness of the LID measures is better for low return periods than moderate and heavy stormwater events. In addition, the LID solutions for peak inundation volume reduction in the flood control source area is more effective than that in the hazard area.

**Ethical Approval** All work is compliance with Ethical Standards.

**Consent to Participate** Not applicable.

**Consent to Publish** The authors are indeed informed and agree to publish.

**Author Contributions** W.Q. conducted the analyses and conceive the manuscript. C.M. completed the numerical simulation and draft the manuscript. H.X. and Z.C. helped to calculate and analyse. K.Z. polished the manuscript. And H.H. helped to recalculate and polish the manuscript in the revision.

**Funding** This study is supported by the National Natural Science Foundation of China (No. 51679156).

**Competing interests** None.

**Availability of data and material** Not applicable (data and material are freely available)**.**

**References**

Ahiablame L, Shakya R (2016) Modeling flood reduction effects of low impact

development at a watershed scale. J Environ Manage 171:81-91. https://doi.org/10.1016/j.jenvman.2016.01.036

Bakhshipour AE, Dittmer U, Haghighi A, Nowak W (2019) Hybrid green-blue-gray decentralized urban drainage systems design, a simulation-optimization framework. J Environ Manage 249: 109364. https://doi.org/10.1016/j.jenvman.2019.109364

Becker P (2018) Dependence, trust, and influence of external actors on municipal urban flood risk mitigation: the case of Lomma Municipality, Sweden. Int J Disast Risk Re 31:1004-1012. https://doi.org/10.1016/j.ijdrr.2018.09.005

Bentley ML, Ashley WS, Stallins JA (2010) Climatological radar delineation of urban convection for Atlanta, Georgia. Int J Climatol 30:1589-1594. https://doi.org/10.1002/joc.2020

Cano OM, Barkdoll BD (2017) Multiobjective, Socioeconomic, Boundary-Emanating, Nearest Distance Algorithm for Stormwater Low-Impact BMP Selection and Placement. J Water Resour. Plann Manage 143: 05016013. https://10.1061/(ASCE)WR.1943-5452.0000726

CHI (Computational Hydraulics Int) (2014). PCSWMM- Advanced Modeling of Stormwater, Wastewater and Watershed Systems Since 1984. Available at: http://www.pcswmm.com/

Cristiano E, Ten Veldhuis MC, Wright DB, Smith JA, Nick VDG (2019) The influence of rainfall and catchment critical scales on urban hydrological response sensitivity. Water Resour Res 55:3375-3390. https://doi.org/10.1029/2018WR024143

555 Duan HF, Li F, Yan HX (2016) Multi-Objective Optimal Design of Detention Tanks in
556 the Urban Stormwater Drainage System: LID Implementation and Analysis. Water
557 Resour Manag 30: 4638-4648. https://doi.org/10.1007/s11269-016-1444-1
558 Fletcher TD, Shuster W, Hunt WF, Ashley R, Butler D, Arthur S, Trowsdale S (2014)
559 SUDS, LID, BMPs, WSUD and more–the evolution and application of
560 terminology surrounding urban drainage. Urban Water J 12:525-
561 542.https://doi.org/10.1080/1573062X.2014.916314
562 Gilroy KL, McCuen RH (2009), Spatio-temporal effects of low impact development
563 practices. J Hydrol 367:228-236. https://doi.org/10.1016/j.jhydrol.2009.01.008
564 Hallegatte S, Ranger N, Mestre O, Dumas P, Corfee-Morlot J, Herweijer C, Muir-Wood
565 R (2011) Assessing climate change impacts, sea level rise and storm surge risk in
566 port cities: a case study on Copenhagen. Clim Change 104:113-137.
567 https://doi.org/10.1007/s10584-010-9978-3
568 Hood MJ, Clausen JC, Warner GS (2010) Comparison of Stormwater Lag Times for
569 Low Impact and Traditional Residential Development. J Am Water Resour As
570 43:1036-1046. https://doi.org/ 10.1111/j.1752-1688.2007.00085.x
571 Huang CL, Hsu NS, Liu HJ, Huang YH (2018) Optimization of low impact
572 development layout designs for megacity flood mitigation. J Hydrol 564: 542–558.
573 https://10.1016/j.jhydrol.2018.07.044
574 Liang CY, You GJY, Lee HY (2019), Investigating the effectiveness and optimal
575 spatial arrangement of low-impact development facilities. J Hydrol 577: 124008.
576 https://doi.org/10.1016/j.jhydrol.2019.124008

577 Liu YZ, Theller LO, Pijanowski BC, Engel BA (2016) Optimal selection and placement
578 of green infrastructure to reduce impacts of land use change and climate change
579 on hydrology and water quality: an application to the Trail Creek Watershed
580 Indiana. Sci Total Environ 553: 149-163.
581 https://doi.org/10.1016/j.scitotenv.2016.02.116
582 Liu. W, Chen WP, Peng C (2014) Assessing the effectiveness of green infrastructures
583 on urban flooding reduction: A community scale study. Ecol Model 291:6-14.
584 https://doi.org/10.1016/j.ecolmodel.2014.07.012
585 Ranger N, Hallegatte S, Bhattacharya S, Bachu M, Priya S, Dhore K, Rafique F, Mathur
586 P, Naville N, Henriet F, Henriet F, Herweijer C, Pohit SJ, Corfee-Morlot J (2011)
587 An assessment of the potential impact of climate change on flood risk in Mumbai.
588 Clim Change 104:139-167. https://doi.org/10.1007/s10584-010-9979-2
589 Salvadore E, Bronders J, Batelaan O (2015) Hydrological modelling of urbanized
590 catchments: a review and future directions. J Hydrol 529:62-81.
591 https://doi.org/10.1016/j.jhydrol.2015.06.028
592 Tang S, Luo W, Jia Z, Liu W, Li S, Wu Y (2016) Evaluating Retention Capacity of
593 Infiltration Rain Gardens and Their Potential Effect on Urban Stormwater
594 Management in the Sub-Humid Loess Region of China. Water Resour Manag 30:
595 983-1000. https://doi.org/10.1007/s11269-015-1206-5
596 Tillinghast E, Hunt WF, Jennings GD, D'Arconte P (2012) Increasing stream
597 geomorphic stability using storm water control measures in a densely urbanized
598 watershed. J Hydrol Eng 17:1381-1388. https://doi.org/10.1061/(ASCE)HE.1943-

599 5584.0000577
600 Urich C, Rauch W (2014) Exploring critical pathways for urban water management to
601 identify robust strategies under deep uncertainties. Water Res 66: 374-389.
602 https://doi.org/10.1016/j.watres.2014.08.020
603 Valizadeh N, Shamseldin, AY, Wotherspoon L (2019) Quantification of the hy
604 draulic dimension of stormwater management system resilience to flooding.
605 Water Resour Manag 33: 4417-4429. https://doi.org/10.1007/s11269-019-023
606 61-1
607 Wang YT, Meng FL, Liu HX, Zhang C, Fu GT (2019) Assessing catchment s
608 cale flood resilience of urban areas using a grid cell based metric. Water
609 Res 163:114852. https://doi.org/10.1016/j.watres.2019.114852
610 Willems P, Arnbjerg-Nielsen K, Olsson J, Nguyen VTV (2012) Climate change impact
611 assessment on urban rainfall extremes and urban drainage: methods and
612 shortcomings. Atmos. Res. 103:106-118.
613 https://doi.org/10.1016/j.atmosres.2011.04.003
614 Williams ES, Wise WR (2006) Hydrologic Impacts of Alternative Approaches to Storm
615 Water Management and Land Development. J Am Water Resour As 42:443-455.
616 https://doi.org/10.1111/j.1752-1688.2006.tb03849.x
617 Winsemius HC, Aerts JCJH, van Beek, LPH, Bierkens MFP, Bouwman A, Jongman B,
618 Kwadijk JCJ, Ligtvoet W, Lucas PL, van Vuuren DP, Ward, PJ (2016) Global
619 drivers of future river flood risk. Nat Clim Change 6:381-385.
620 https://doi.org/10.1038/nclimate2893

621 Xu HS, Ma C, Lian JJ, Xu K, Chaima E (2018) Urban flooding risk assessment based
622 on an integrated k-means cluster algorithm and improved entropy weight method
623 in the region of Haikou, China. J Hydrol 563:975-986.
624 https://10.1016/j.jhydrol.2018.06.060
625 Xu T, Jia HF, Wang Z, Mao XH, Xu CQ (2017) SWMM-based methodology for block-
626 scale LID-BMPs planning based on site-scale multi-objective optimization: a case
627 study in Tianjin. Front Env Sci Eng 11: 48-59. https://doi.org/10.1007/s11783-
628 017-0934-6
629 Zischg J, Goncalves MLR, Bacchin TK, Leonhardt G et al (2017) Info-Gap robustness
630 pathway method for transitioning of urban drainage systems under deep
631 uncertainties. Water Sci Technol 76: 1727-1281.
632 https://doi.org/10.2166/wst.2017.320

# Figures

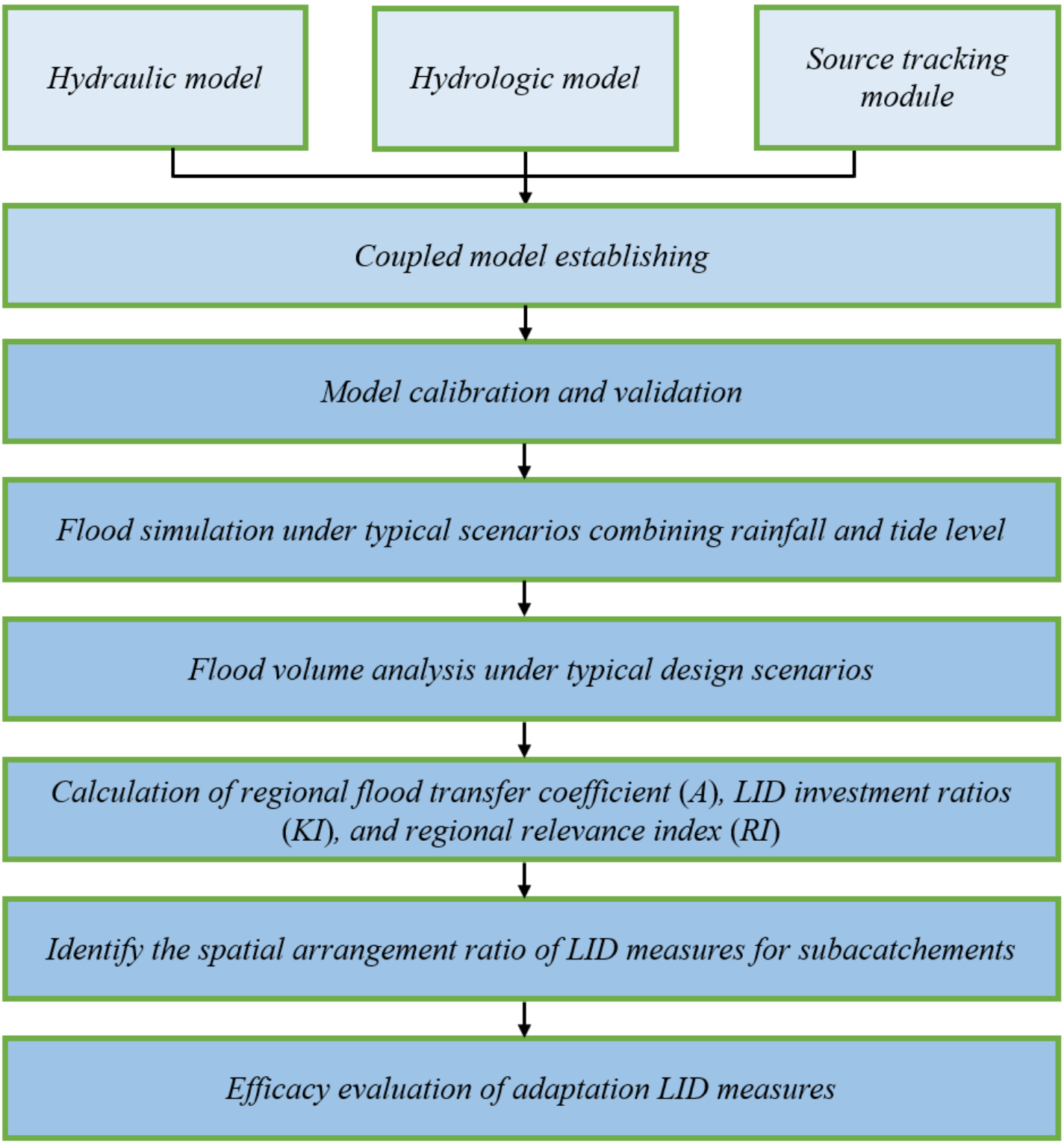


**Figure 1**

Optimal framework of spatial arrangement of low impact development (LID) measures based on source tracking for urban flood mitigation


## Figure 2

Schematic diagram of the runoff source tracking process in urban watershed

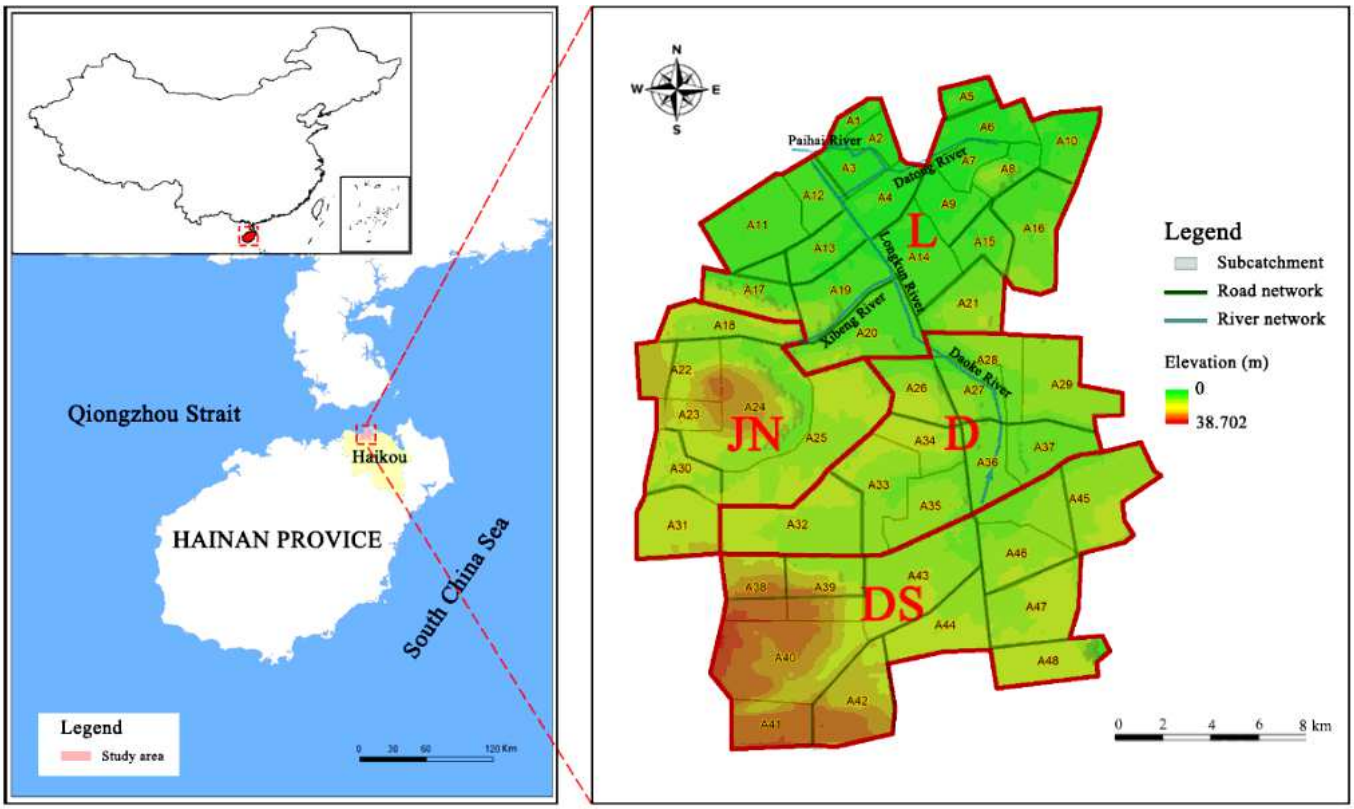

Figure 3

Study area and sewer system distribution Note: The designations employed and the presentation of the material on this map do not imply the expression of any opinion whatsoever on the part of Research Square concerning the legal status of any country, territory, city or area or of its authorities, or concerning the delimitation of its frontiers or boundaries. This map has been provided by the authors.

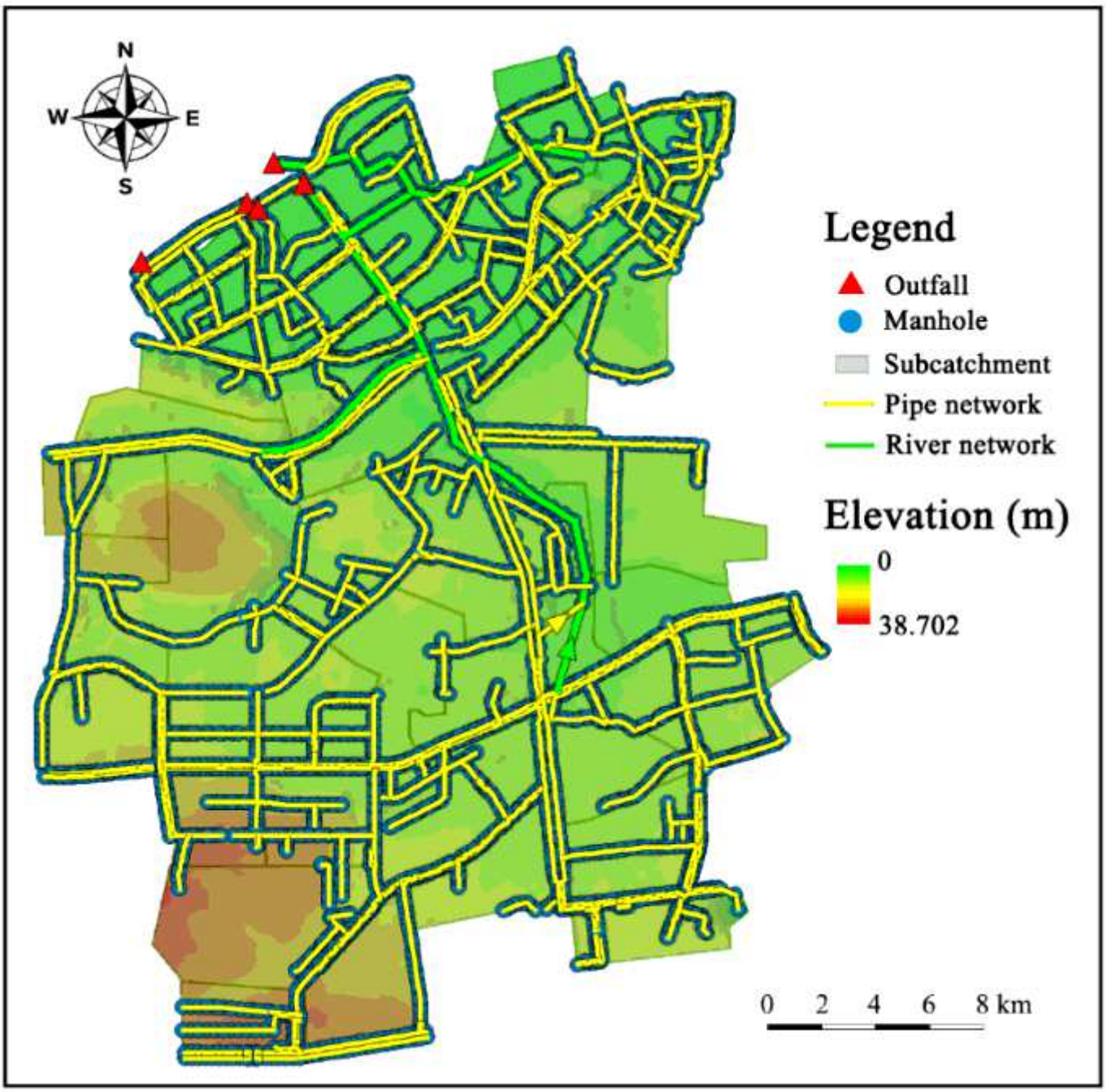


Figure 4

Urban flood model establishing of study area based on the PCSWMM Note: The designations employed and the presentation of the material on this map do not imply the expression of any opinion whatsoever on the part of Research Square concerning the legal status of any country, territory, city or area or of its

authorities, or concerning the delimitation of its frontiers or boundaries. This map has been provided by the authors.

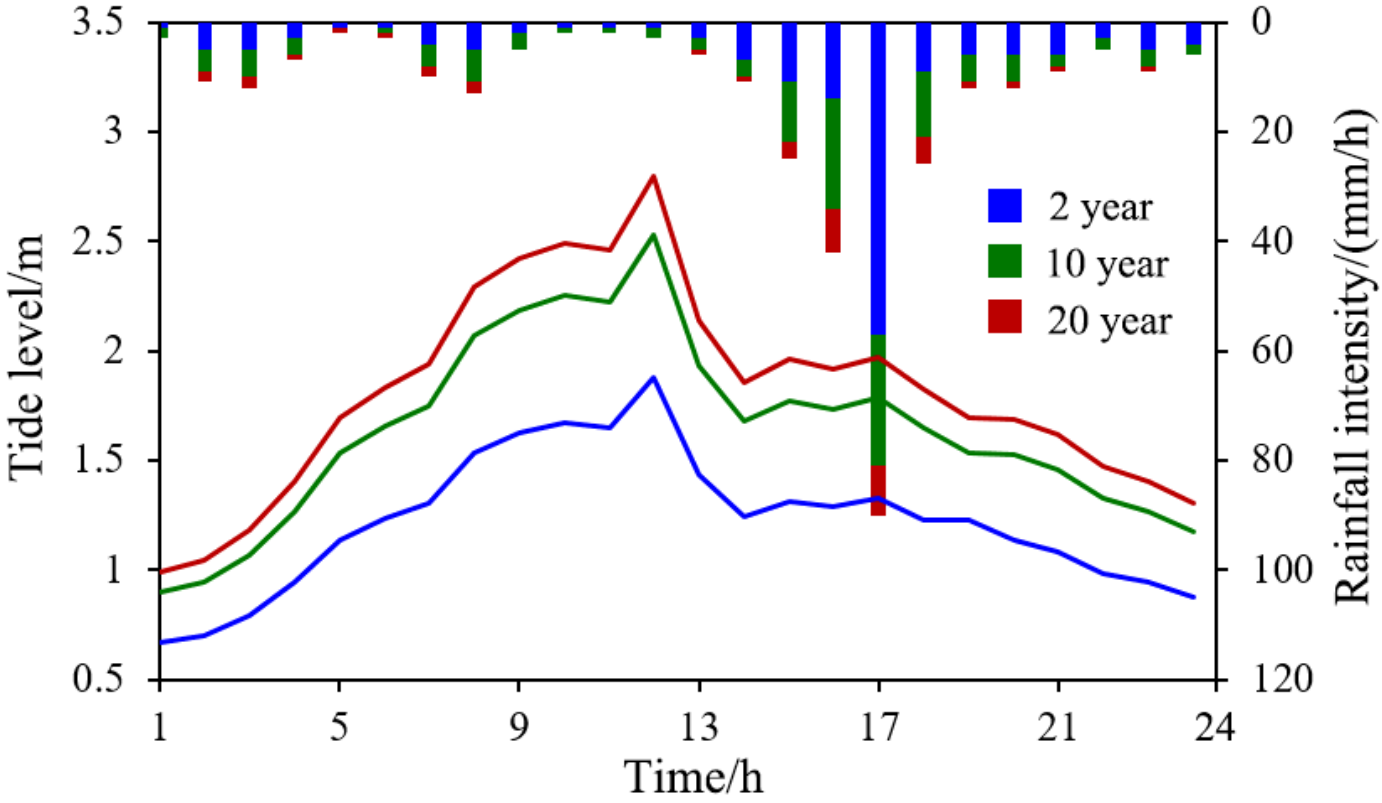


**Figure 5**

Distribution of design rainfall and tide level

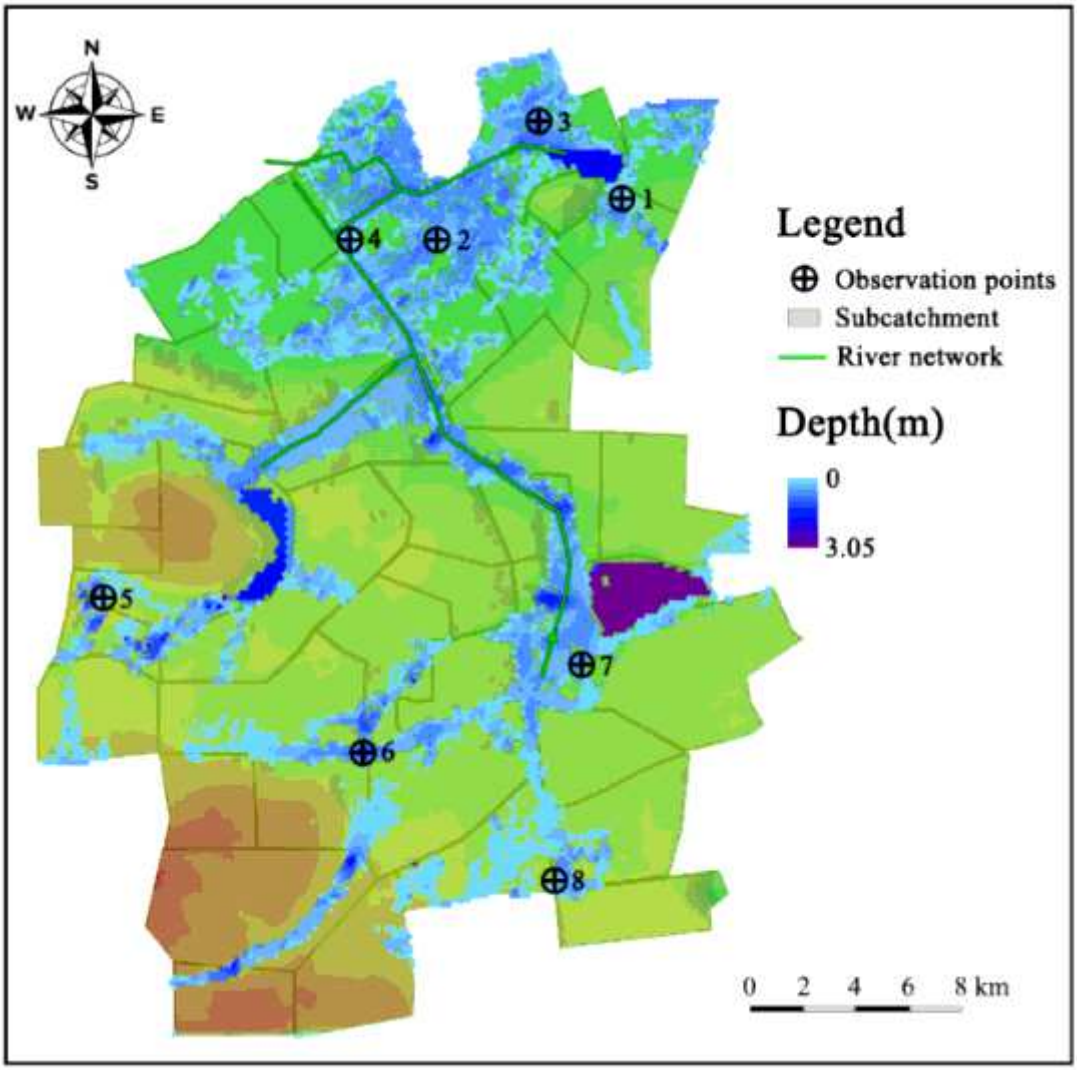


**Figure 6**

Simulation flood during the “Rammasun” typhoon storm event in July 2014 Note: The designations employed and the presentation of the material on this map do not imply the expression of any opinion whatsoever on the part of Research Square concerning the legal status of any country, territory, city or area or of its authorities, or concerning the delimitation of its frontiers or boundaries. This map has been provided by the authors.

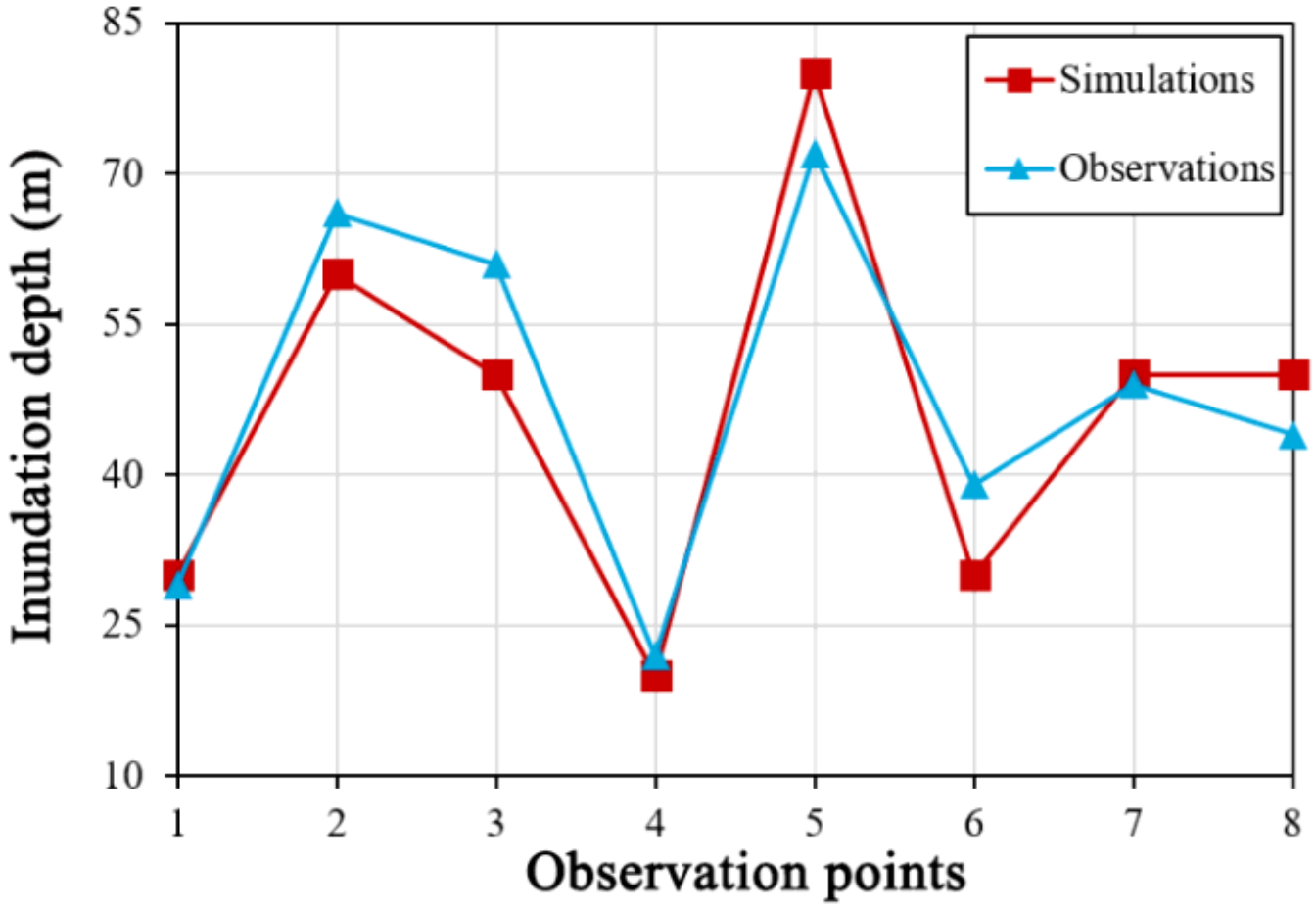


**Figure 7**

Calibration of the PCSWMM

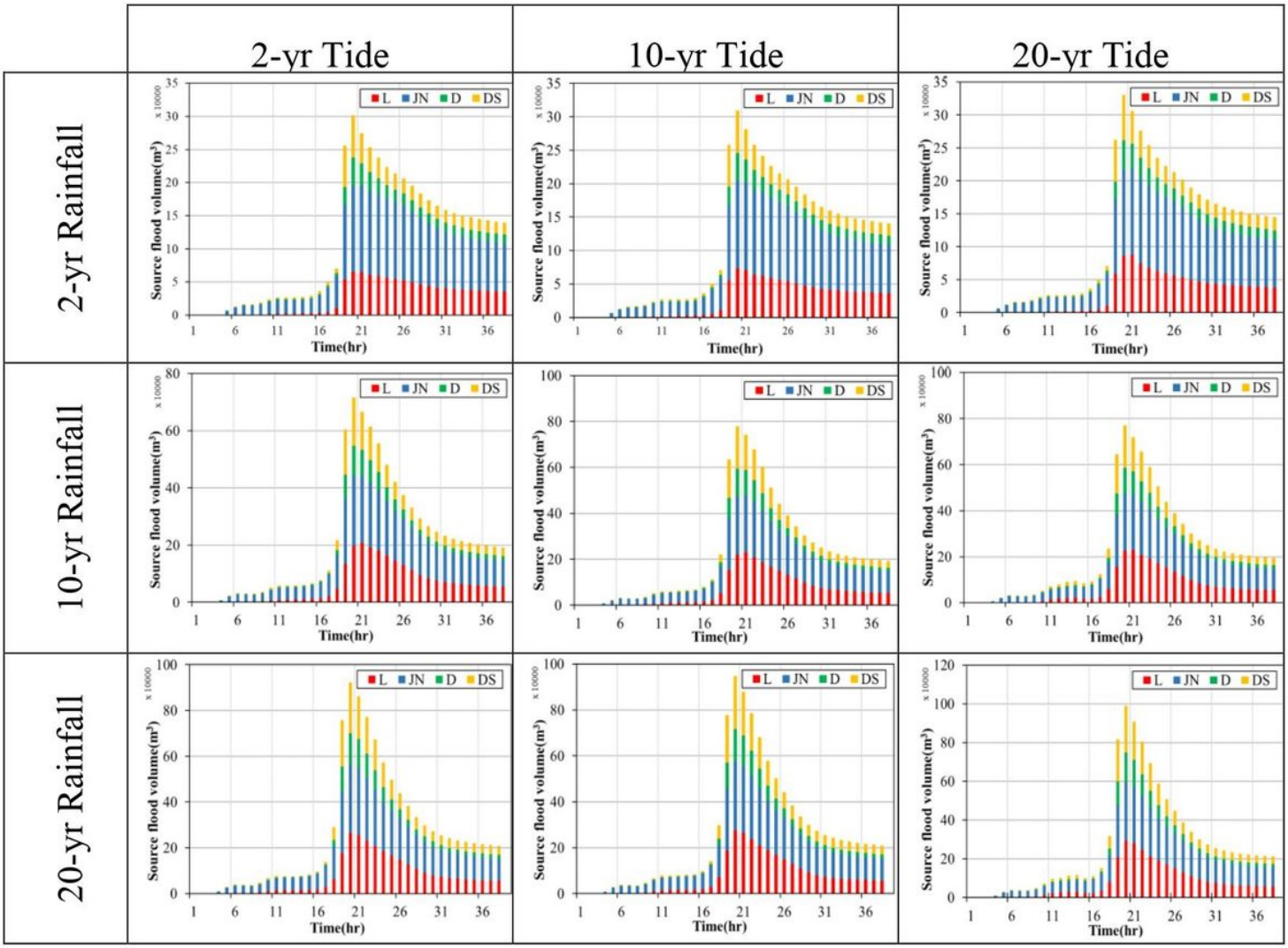


**Figure 8**

Diagram of flood source area inundation volume contribution to hazard area under the combined impact of storm tides and heavy rainfall

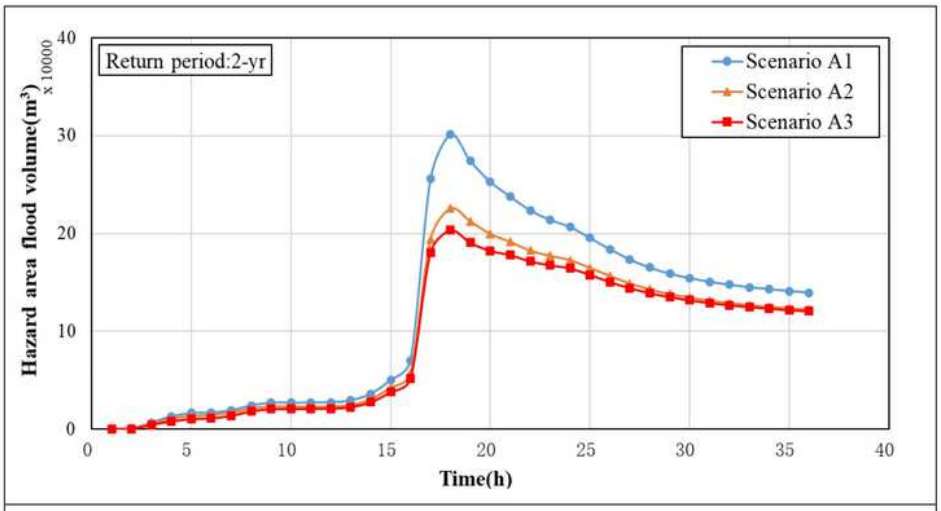


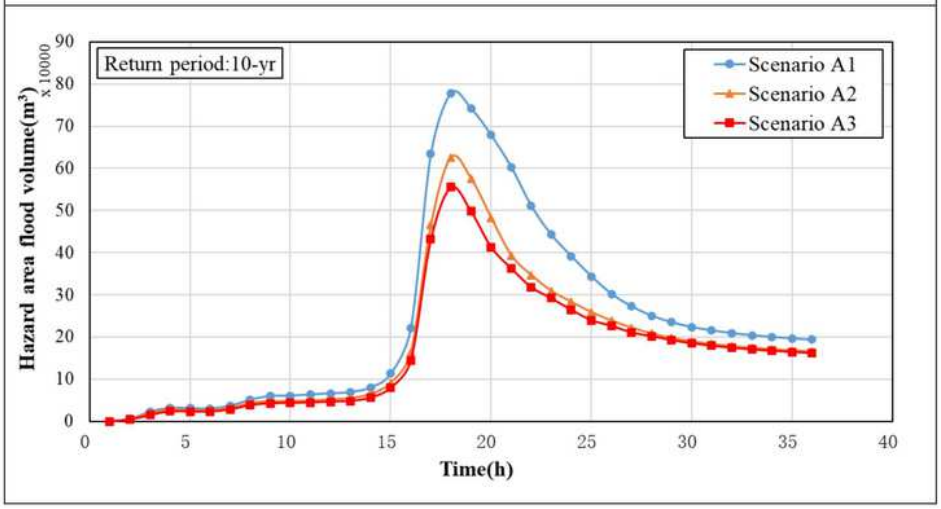


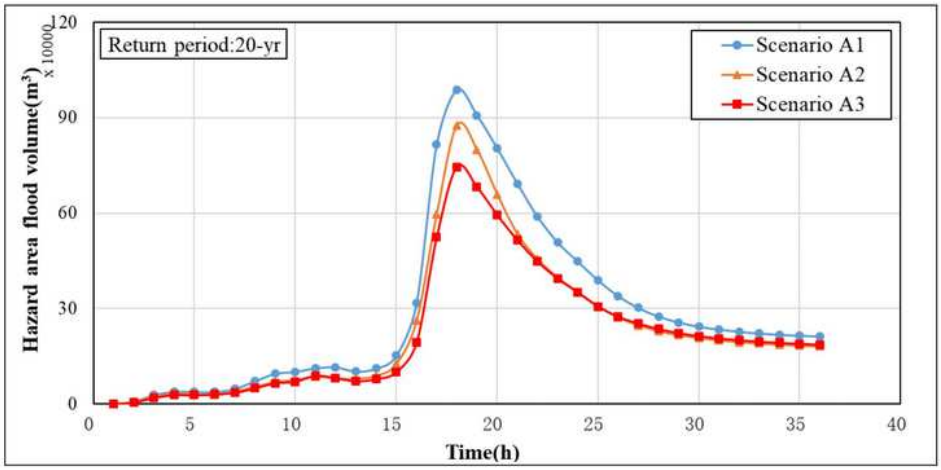


## Figure 9

Comparative diagram of inundation volumes in three scenarios during combined storm tide and heavy rainfall